Renewable Additives that Improve Water Resistance of Cellulose Composite Materials

Heather L. Buckley, Caitlin H. Touchberry, Jonathan P. McKinley, Zachary S. Mathe, Hurik Muradyan, Hannah Ling…Susan E. Amrose

2016

Renewable Additives that Improve Water Resistance of Cellulose Composite Materials

Heather L. Buckley[1]*, Caitlin H. Touchberry[2], Jonathan P. McKinley[2], Zachary S. Mathe[1], Hurik Muradyan[1], Hannah Ling[2], Raj P. Fadadu[1], Martin J. Mulvihill[1] and Susan E. Amrose[2]

[1]*Berkeley Center for Green Chemistry, University of California Berkeley, Berkeley, California 94720*
[2]*Civil and Environmental Engineering, University of California Berkeley, Berkeley, California 94720*

Received February 22, 2016; Accepted April 19, 2016

ABSTRACT: Waste cardboard is an underutilized resource that can be redirected for the creation of safer and higher quality building materials for low-income housing in the developing world, as well as to produce better materials for indoor environments in developed-world contexts. Using a renewable biobased binder and benign additives, we have improved the water resistance of a cardboard-based composite material, overcoming one of the major barriers to scaling and adoption of this class of materials. Resistance to water uptake was significantly increased with several additives and was increased over 900-fold in the best case. Strength and water uptake over time are reported for a range of fatty acid-based additives and multiple cardboard feedstocks.

KEYWORDS: Renewable biobased additives, waste valorization, water repellency, cellulose composite materials, green chemistry

1 INTRODUCTION

According to the 2011 census, over 65 million people in India live in dwellings deemed unfit for human habitation, often referred to as slums [1]. Worldwide, the estimated population living in slums was almost 1 billion people in 2006 and is expected to reach 1.4 billion by 2020 [2]. Slum dwelling walls are typically built with bricks, which are adequate for exterior walls, but thick inner walls have a significant footprint and preclude the inclusion of separated sanitation in small spaces. Roofs are constructed from low quality corrugated metal or asbestos cement, which provide inadequate thermal and sound insulation and require frequent repair. The best available alternative material, pre-cast concrete slab, is expensive and cannot be transported through narrow alleyways or on rural roads. Additionally, the potential negative health impacts of many products available in the developing world, including asbestos cement sheets and a variety of plastics, are a serious concern [3, 4]. Many of these materials, along with composites that release potential carcinogens and asthmagens, are widely used in developed-world contexts as well. There is a need for new affordable and durable materials with a lower environmental impact and reduced health risk for roofing, flooring, interior walls, and toilet superstructures in both rural and urban contexts.

Every year, 500 billion USD worth of cardboard is produced on a global scale [5]. Two thirds of this market is comprised of corrugated and solid fiber boxes, with the residual made up of food containers and various paperboard products. While a small amount of this material is recycled or downcycled for reuse, the vast majority is either disposed in a landfill or burned. Both of these endpoints retain little of the original value of the waste cardboard and result in CO_2 emissions and the pollution of air or groundwater.

Given the scale on which cardboard is produced and discarded, there is an opportunity to convert cardboard waste into composite building materials. Composed primarily of cellulose, cardboard contains fibers that have been thoroughly processed to remove lignin but maintain the strength and flexibility of the cellulose polymer. Cardboard pulp is ideal for incorporation into bulk materials because the fibers can be properly dispersed to interact with a binder in a homogeneous manner. Similarly, processed softwood fiber has been extensively explored for use in fiber-reinforced cement as a safer alternative to asbestos [6, 7] and as a replacement for glass and other fibers in resin-based composites [8]. While

*Corresponding author: hbuckley@berkeley.edu

DOI: 10.7569/JRM.2016.634109

fibers from cardboard tend to be shorter than those of virgin softwood pulp, there are many environmental advantages of valorizing waste rather than processing a virgin material, particularly considering the energy-intensive nature of the Kraft pulping process [9]. Well-designed, locally sourced and manufactured materials have the potential to improve quality of life in slum dwellings and formal housing contexts while reducing the negative environmental and health impacts associated with current options.

A number of research groups and commercial ventures have taken the approach of valorizing fibrous waste by using cardboard [10–12], and in some cases straw [13, 14], as a bulk material in construction or in packaging. Preliminary tests indicate that this sort of composite has reasonable mechanical properties. However, several technical obstacles must be overcome to develop a composite cardboard-based material that is more environmentally friendly, improves quality of life, and is locally affordable. First, most fiber-based materials, such as particleboard, are held together by organic polymeric resins; these typically contain formaldehydes and have been demonstrated to off-gas volatile organics that are known carcinogens and can cause skin and respiratory sensitization and irritation [4]. Buildings constructed with traditional materials release chemicals that contribute to indoor air pollution [15, 16]. In some cases formaldehyde from fiberboard has been directly linked to occupant illness [17]. However, alternative binders are a possibility. Cement, mentioned previously, solves many toxicity problems, but has high embodied energy and the caustic environment can cause degradation of cellulose fibers and negatively impact mechanical performance [7, 18]. Biobased binders, such as starches that are byproducts of grain processing, offer a viable alternative but are not as well studied.

A second more challenging obstacle is the high level of water absorption of cardboard. If full waterproofing is required (e.g., for outdoor applications), then several commercial coatings, including epoxy, polyurethane, and other proprietary options, are available and widely used in the building industry. However, relying on a coating for waterproofing leaves the material vulnerable to cracks or holes made in that coating, allowing water to enter the cardboard core and causing the cardboard to swell.

A range of chemical [19] and mechanical [20, 21] methodologies has been used to successfully impart hydrophobicity into cellulosic fibers. These are generally of limited use in the context of making a bulk material waterproof; the goal of most research in this area has been to improve interfacial binding between relatively polar cellulosic reinforcement additive and a nonpolar matrix or bulk material. For example, in cement, cellulose fibers provide a safer alternative to asbestos fibers from a health perspective [7], and in polymer/resin-based composites, they provide a biobased alternative to glass or petroleum-based synthetic fibers [8].

In addition to the fact that they are not optimized for imparting bulk hydrophobicity on a material, many of the chemical processes used to change the polarity of cellulose do not embody the principles of green and sustainable chemistry and engineering, namely the design and production of materials in a way that minimizes harm to human health and the environment throughout the entire product life cycle [22]. Their applications in a process intended to generate composites that are safer than existing technologies are therefore limited.

In particular, potentially hazardous chemicals (isocyanates, organohalogen compounds) and harsh conditions (extractions at high temperatures in a range of organic solvents) are common in cellulose modification. Methods to improve the water resistance of cellulose fibers found in the literature typically involve covalent reactions and either "masking" with small functional groups [23–25], crosslinking and copolymerization [26–29], or a combination of the two [30, 31]. The potentially hazardous or harsh conditions employed in established methods are outlined in Table S1.

If a somewhat polar biobased binder is used rather than a nonpolar polymer or cementitious material, then the covalent attachment of water-repellent molecules to cellulose may not be necessary for the cohesiveness of the material. Rather, it may be sufficient to incorporate a biobased amphiphilic molecule to impart hydrophobicity through a noncovalent interaction with cellulose. For comparison, examples exist where silica nanoparticles are successfully incorporated noncovalently into a fiber matrix [32]. Hydrogen bonding may provide sufficient interaction between the cellulose and the hydrophilic end of a molecule, while the hydrophobic end provides water resistance. Specifically, long-chain fatty acids and their salts are readily available amphiphilic molecules that have low toxicity. The broad vision of this choice is to continue the theme of valorizing waste products either through the saponification of used cooking oils or through use of stearates, which are a byproduct of the slaughtering industry. Stearic acid is a more readily studied fatty acid source because it is commercially available in pure form. Stearates are broadly used as lubricants, meaning that they have been commoditized, so their use at scale would not introduce some of the challenges associated with large-scale collection of waste oils.

In this article, we analyze the impact of adding stearate salts on the water resistance and strength of a pulped cardboard-cornstarch composite material that is pressed into a panel and dried. The intended end-use of this material is as a building material made from valorized waste and low-value products for use in such contexts as flooring, non-load-bearing interior walls as an alternative to plywood or MDF, or as a coated single-layer roofing material as an alternative to metal or asbestos cement sheeting. We explore the differences between several methods of incorporation of stearate additive to understand practical process implications in a factory setting and compare its efficacy to that of oleic acid, the *cis*-monounsaturated analogue of stearic acid, which is a liquid at room temperature. These variants of the material, along with samples without additives, are compared by way of water uptake upon immersion of small samples cut from manufactured panels. Additionally, the strength of the material with and without additive is compared with some standard non-load-bearing materials. The combined results of these tests provide an indication of reasonable applications for this new material for use in the built environment. This material does not contain formaldehydes or other harmful volatile organic compounds (VOCs), is sourced from waste and byproducts and so does not contribute to resource extraction and exploitation, is biobased and will degrade readily at its end-of-life, and is a potentially suitable alternative building material panel for a range of applications in development and conventional built environment contexts.

2 MATERIALS AND METHODS

2.1 Materials Used in Fabrication of Samples

Cardboard, or paperboard was sourced from one of three places:

- Paper plate factory in GIDC Vatwa, Ahmedabad, India. This material is leftover after cutting disposable plates from large reams of non-corrugated paperboard. This material is referred to as "India Paper" throughout the text and Supporting Information.
- Regular unbleached North American corrugated cardboard from shipping boxes (such as those provided by Sigma Aldrich). This material is referred to as "US Cardboard" throughout the text and Supporting Information.
- Chinet brand paper plates "Classic White" purchased off the shelf in Berkeley, CA. This material is referred to as "US Plate" throughout the text and Supporting Information.

Cornstarch was purchased from local industrial food suppliers.

Coconut fiber was obtained from local suppliers in Ahmedabad, India.

Sodium stearate, calcium stearate, oleic acid, calcium hydroxide, hydrochloric acid, and calcium chloride were purchased from chemical suppliers and used as received.

Epoxy and hardener were purchased from local coatings suppliers and combined and used as directed on the packaging.

Birch plywood, bullnose MDF (medium-density fiberboard), and regular MDF used for material strength comparisons were purchased from a hardware store in Berkeley, CA.

2.2 Sample Preparation

Sample preparation took place in two facilities by very similar methods as described below.

Method A: For each m^2 of final panel, 23.0 kg cardboard strips were weighed and soaked in water for 24 to 48 h to saturate and begin dispersing the fibers. The soaked cardboard was then transferred from the water to an industrial food processor, keeping enough water in the mixture to facilitate blending into a uniform pulp. The pulp was transferred to an upright cement mixer of appropriate size. At this point, additives were introduced to the mixture as described in Table 1, mixing between each added component. Following the incorporation of additives, 12.3 L of a 33% wt/wt homogeneous suspension of cornstarch in near-boiling water was mixed into the pulp, and 270 g/m^2 coconut fiber was added. The material

Table 1 Additive compositions (in amount per m^2 of final dried panel).

Sample name	Sample description	Sample details
Control	Control, no additive	No additive
NaSt	Sodium stearate/HCl/$Ca(OH)_2$	3.68 kg/m^2 sodium stearate, 12.65 mol/m^2 hydrochloric acid, 486 g/m^2 calcium hydroxide
CaSt	Calcium stearate added directly	3.68 kg/m^2 calcium stearate
OleH	Oleic acid	3.68 kg/m^2 oleic acid
CaOle	Oleic acid/$Ca(OH)_2$	3.68 kg/m^2 oleic acid, 486 g/m^2 calcium hydroxide

was transferred into a mold of appropriate size and pressed with approximately 4.3 MPa (45 tonnes/ft^2) for roughly 45 minutes. The resulting panel was dried in an oven at 80–120 °C until the weight of the panel matched the sum of the original dry components to within 5% (typically 48–72 h).

Method B: Using the same quantities per m^2 as in Method A, cardboard was weighed, torn into 1.5 foot squares, and soaked in water overnight to saturate and begin dispersing the fiber. The cardboard was then torn into 4 inch strips. In batches, these strips were mixed with an adequate amount of water in a food processor on high speed. In this way, the material was reduced to a pulp with no distinct sheets of cardboard visible. The resulting slurry was squeezed between two perforated colanders to remove excess water. At this point, additives were added as described in Table 1, mixing between each added component. In a mixer, the slurry and coconut fibers (pre-cut into 3 cm lengths) were combined in alternating portions until all of the slurry and fibers had been added. A suspension of cornstarch in water heated to 60 °C, mixed carefully to avoid clumps, was added to the mixture, and the material was blended with a dough hook on medium-low speed until the cornstarch mixture was fully incorporated. The material was then scooped into a mold of appropriate size lined with wire mesh and vegetable oil to prevent the material from sticking and pressed with approximately 4.3 MPa (45 tonnes/ ft^2) for roughly 20 minutes. The resulting panel was dried in an oven at 110 °C until the weight of the panel matched the sum of the original dry components to within 5%.

All panels were cut into 50 mm × 50 mm samples for water immersion testing and 305 mm × 152 mm samples for strength testing. Samples from the outer 50 mm perimeter of each pressed panel, as well as any sample showing visible cracks on any face, were rejected from the testing set. Throughout the text, samples are referred to by their cardboard feedstock and additive content, for example, "India Paper-CaOle" is a sample made from the Indian paper plate cardboard feedstock that contains the calcium oleate additive.

Oleic Acid Dipping of Samples – Some 50 mm × 50 mm samples were dipped in oleic acid or first oleic acid and subsequently a saturated aqueous solution of calcium chloride. The oleic acid was heated to ~50 °C, and the sample was fully immersed for 2 s then allowed to drip dry for 15 s. If the sample was subsequently dipped in saturated $CaCl_2$ solution, this occurred immediately; the sample was fully immersed in the aqueous solution for 2 s. In both cases, samples were then allowed to fully dry overnight or longer at room temperature before any further testing.

Epoxy Coating of Samples – Some samples were coated in epoxy and then scored on one face (see Figure 4a). In all cases, the epoxy was mixed according to the manufacturer's directions, and then applied to the samples with a paintbrush. Three coats were applied to each sample, waiting for each coat to dry but not fully cure. A ~2 mm deep cut that extended through the coating and exposed uncoated material was made into one of the 50 mm × 50 mm faces of each sample across the center of that face.

2.3 Water Uptake Measurement during Immersion of Samples

All samples were weighed when dry and equilibrated to ambient indoor conditions in Berkeley, California (~22 °C, 50–75% humidity). Samples were subsequently immersed in water, using weights to keep them submerged because all samples float in water initially. Masses were obtained on a Mettler Toledo PL203 top-loading balance (210 × 0.001 g ± 0.002 g) after 5 min, 10 min, 30 min, 1 h, 4 h, 8 h, 24 h, and daily beyond that time. Samples were removed from testing once they had reached 1.5 times their original mass. Epoxy-coated samples were tested at the same intervals; sampling frequency was reduced to 72–168 hours after two months.

2.4 Data Analysis for Water Uptake Tests

Raw data of mass as a function of time for each sample was divided by the original (dry) sample mass to give a ratio relative to original mass. From these ratios, we determined the last recorded time at which each sample remained below mass thresholds of 1.05 (5% mass gain), 1.10 (10% mass gain), 1.20 (20% mass gain), 1.30 (30% mass gain), 1.40 (40% mass gain) and 1.50 (50% mass gain), as well as the first time the mass exceeded 1.50 (50% mass gain), which was considered to constitute "failure," marking the end of the experiment for each sample. For samples that gained a large amount of mass before the first data collection, we recorded a time of 0.001 hours to simplify computerized statistical analysis.

To compare among treatments (Control, NaSt, CaSt, OleH, CaOle, samples dipped in oleic acid, samples dipped in oleic acid/$CaCl_2$) and cardboard feedstocks (US Cardboard, India Paper, US Plate), t-tests were run comparing the groups of data for each treatment at each level of mass gain (less than 5%, 10%, 20%, 30%, 40%, 50%, and greater than 50%). In nearly all cases, an F-test revealed that standard deviations were significantly different between samples, so degrees of freedom and t-values for each comparison were determined using general-case equations [33]. Treatments were considered to have significantly different

outcomes if they passed the t-test at a 95% or greater confidence level.

2.5 Water Droplet Interactions with Material Surface

The behavior of single water drops on the surface of small panels was investigated using digital photography. These panels were prepared by the same procedure as outlined in Section 2.2, but in ~10 cm × 10 cm samples and with no additive, 2.13 kg/m^2, or 2.89 kg/m^2 sodium stearate (along with the corresponding quantities of hydrochloric acid and calcium hydroxide to maintain the same ratios as in Table 1) as part of an early rapid-screening process. A device similar in principle to a basic contact angle measurement goniometer, such as the DataPhysics OCA 15EC [34, 35], was constructed using a Canon PowerShot A430 digital camera, a ring stand and clamps. A sample was placed on a slide, which was manually tilted to make the sample surface parallel to the optical axis. A water droplet was dispensed from a Pasteur pipette positioned just high enough above the sample such that the drop would not remain adhering to the pipette after falling onto the sample surface. Drops were dispensed onto flat and uniformly textured portions of panel samples. The 4-megapixel camera, using 2–3x optical zoom and "Super Macro" mode, was used to capture images of the water-surface interface at 1 s, 5 s, 20 s, and 20 min after the release of the droplet.

2.6 Strength Testing by Four-Point Test

Strength testing of the cardboard composite materials, and of other materials for comparison, was conducted by way of a four-point bending test in accordance with the ASTM D6272-10 Standard Test Method, which is applicable for rigid and semi-rigid composites in the form of rectangular bars. Samples (305 mm × 152 mm) were marked at the center to assist in measuring deflection during testing. Additional lines were added to mark the placement of the loading noses and supports of the four-point bending fixture.

The samples were tested in a Baldwin Universal Testing Machine (UTM) with a maximum capacity of 24 kips (107 kN). Each sample was placed on two bottom supports before two upper supports and a swivel head were rested symmetrically on top of the sample. For each of the bottom and top pairs of supports, one was a point load support able to swivel, and the other was a line load support, which remained fixed. The load span length at 76 mm, or distance between the two loading points, was one third of the support span length at 229 mm. The radii of the support loading noses were 6 mm.

The UTM was set to a constant deflection rate of 0.018 inches/minute (0.46 mm/minute). A linear variable differential transformer (LVDT) was placed beneath the center of the tile to measure the maximum deflection of the sample in real time, while LabVIEW© software [36] recorded and graphed this deflection as well as the load from the UTM. The tests proceeded uninterrupted beyond the point where a distinct maximum flexural load was reached as indicated on the LabVIEW load-deflection graph. Strength tests were halted when fractures became visible on the surface of the test sample between the upper supports. One sample that showed signs of failure outside the center third of its geometry was removed from the data set due to inconsistencies in its material properties.

From the maximum load and deflection data, modulus of rupture (MOR) and bending modulus of each sample were calculated [37]. Multiple samples were run for each treatment, and the grouped data were compared by way of a t-test. In nearly all cases, an F-test revealed that standard deviations were significantly different between samples, so degrees of freedom and t-values for each comparison were determined using general-case equations [33]. Treatments were considered to have significantly different outcomes if they passed the t-test at a 95% or greater confidence level.

3 RESULTS AND DISCUSSION

3.1 Water Resistance/Immersion Tests

In initial experiments, samples were prepared with sodium stearate/HCl/$Ca(OH)_2$ (referred to as "NaSt" throughout) as additives to determine the influence of these additives on hydrophobicity and water uptake. Sodium stearate is partially soluble in water and can be readily incorporated in the slurry of cardboard material. The sodium stearate was acidified to improve solubility and interactions with the cardboard using a slight excess of hydrochloric acid (Equation 1). Calcium hydroxide was subsequently added to form the insoluble calcium stearate salt (Equation 2). These initial tests showed a significant difference in water uptake between control panels (those with no additive) and those containing the NaSt/HCl/$Ca(OH)_2$ additive (Figure 1; numerical data for all graphs can be found in the Supporting Information).

$$C_{17}H_{35}COONa + HCl \rightarrow C_{17}H_{35}COOH + NaCl \quad (1)$$

$$2C_{17}H_{35}COOH + Ca(OH)_2 \rightarrow (C_{17}H_{35}COO)_2Ca + 2H_2O \quad (2)$$

Working at a large scale in a factory setting means that each step of measurement and addition impacts

 DOI: 10.7569/JRM.2016.634109

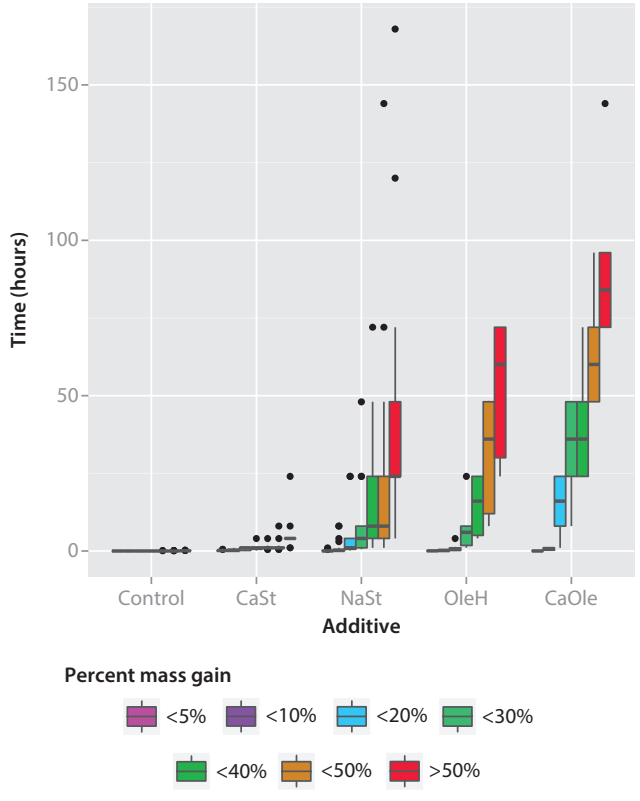

Figure 1 Mass increase vs. immersion time of 50 mm × 50 mm samples including a Control and NaSt, CaSt, OleH, and CaOle additives. Boxplots for each level of mass gain (denoted by color) and each additive treatment (grouped, labeled on x-axis) show median (line), second to third quartiles (box), most extreme data point within 1.5 × the interquartile range (whiskers), and outliers (black dots).

the time needed for the process and therefore potentially the cost and/or the exposure of workers to the material in use. To determine whether water resistance was affected by the use of calcium stearate directly as a powder vs. calcium stearate prepared indirectly by the addition of sodium stearate/HCl/$Ca(OH)_2$, samples were prepared using calcium stearate directly. The procedure beginning with sodium stearate produced samples with significantly longer immersion time before failure (Figure 1). This graph demonstrates both the improved performance of tiles based on additive and the large amount of variance between their performances. The high level of variability in performance is likely a result of a small-scale manufacturing process; specifically the degree of compression of material during pressing and inconsistencies in drying temperature may cause variation between pressed panels, and samples from nearer to the edges of a particular panel to be lower in density or have microscopic cracks that allowed water penetration.

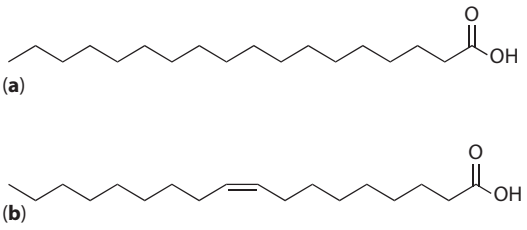

Figure 2 Structures of (**a**) stearic acid and (**b**) oleic acid.

The difference in performance between NaSt/HCl/$Ca(OH)_2$ and direct $CaSt_2$ additives may be explained by poor dispersion of calcium stearate within the slurry while preparing these samples. Calcium stearate powder is so hydrophobic that, even when wet, it puffs up as a powder above the cement mixer, while sodium stearate "wets" and becomes better incorporated into the mixture. The extreme hydrophobicity of the calcium stearate powder meant that this material was in fact quite difficult to work with in an industrial setting, as it mixed poorly with the pulp and tended to coat surrounding surfaces in fine white dust. While it is a low toxicity compound, which means a single exposure is not of great concern from a worker health and safety perspective, repeated exposure to fine particulates of this material could potentially cause respiratory irritation and related chronic issues [38]. When choosing a waterproofing additive that is benign throughout its lifecycle, this is a serious concern, and so both the properties of calcium stearate itself and the lower performance of the composite containing calcium stearate suggest that it is a poor choice in this context.

Recognizing that working with any powder, even one less challenging to manipulate than calcium stearate, may have both practical and health and safety concerns at a large scale, a fully liquid alternative additive was investigated. Oleic acid is an 18-carbon carboxylic acid and a *cis*-monounsaturated analogue of stearic acid. The unsaturation in the long fatty acid tail introduces a "kink" which decreases the strength of van der Waals forces between molecules, and as a result, oleic acid is a liquid at room temperature, while stearic acid is a solid (Figure 2). While there are potential durability issues surrounding the oxidation and degradation of oleic acid, it is the liquid fatty acid that should provide the closest behavior to stearic acid in terms of hydrophobicity.

Samples were prepared containing either oleic acid or oleic acid and subsequently $Ca(OH)_2$ to form the calcium oleate salt (OleH and CaOle, respectively, Figure 1). CaOle samples performed significantly better than corresponding OleH and NaSt samples. There was no significant difference in the behavior of

OleH and NaSt samples, suggesting that a combination of greater dispersion of the liquid fatty acid (as compared to a partially soluble powder in the case of NaSt) and hydrophobicity of the final calcium salt (as compared to the free acid) both contribute to the better water resistance of CaOle samples.

An alternate mode of incorporating oleic acid into samples was also explored. Fully prepared, dried, and cut material samples were dipped in oleic acid for several seconds and then allowed to dry. This was done both with oleic acid and with oleic acid followed by a saturated aqueous solution of calcium chloride to allow substitution of the acid group with a less soluble calcium counterion. The data for this experiment is shown in Figure 3. While both conditions of dipped samples perform significantly better than the Control, there is no significant difference in performance between samples dipped only in oleic acid and those subsequently dipped in calcium chloride solution. For most levels of mass increase, there is also no significant difference between either type of dipped samples and NaSt additive samples, although the samples with additive do take significantly longer to reach 5% mass gain than either type of dipped sample. CaOle samples take significantly more time to reach 20, 30, 40, and 50% mass gains than either type of dipped samples, suggesting that incorporation of an additive is a more effective means of imparting water resistance than dipping the material in the additive after pressing and drying.

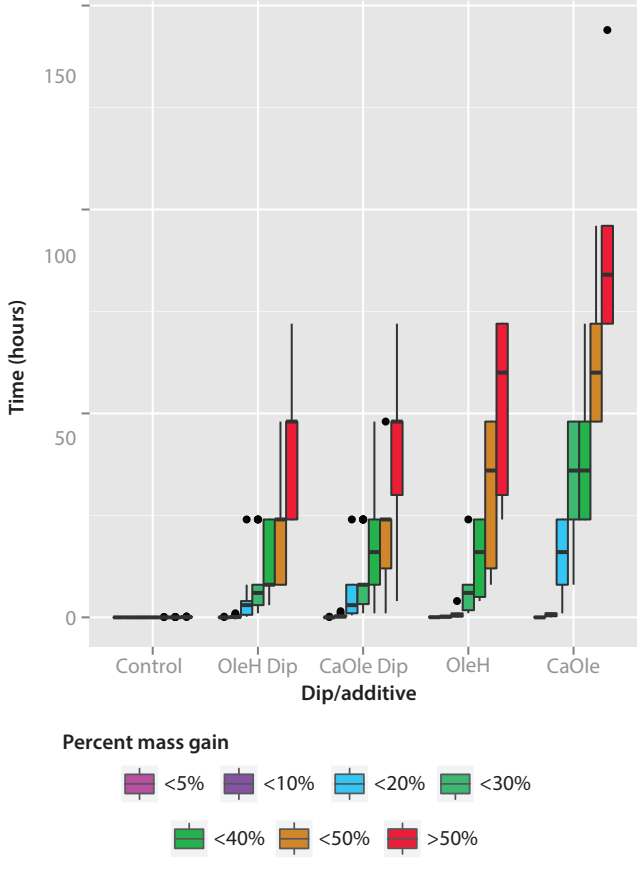

Figure 3 Mass Increase vs. immersion time of 50 mm × 50 mm samples containing no additive that have been dipped in nothing (Control), oleic acid or oleic acid and calcium chloride, as well as samples containing OleH or CaOle additive. Boxplots for each level of mass gain (denoted by color) and each additive treatment (grouped, labeled on x-axis) show median (line), second to third quartiles (box), most extreme data point within 1.5 × the interquartile range (whiskers), and outliers (black dots).

The above immersion experiments provided a surrogate for the "worst case scenario" of water exposure of a building material. In most applications, bulk materials would be covered with some kind of coating (either paint or a more robust outer shell), often providing a great deal of water repellency. To simulate the situation where our building material has a waterproof coating, but is compromised by a crack or scratch, samples containing all of the different additives discussed above were coated with epoxy. A controlled point of failure was introduced by way of a ~2 mm deep cut along one of the faces of the sample, exposing the cardboard beneath the coating (see Figure 4). These samples were then tested for water resistance by soaking in the same manner as those not coated with epoxy.

The results of water resistance tests for epoxy-coated NaSt, CaSt, OleH, and CaOle samples are shown in Figure 5. All additives except CaSt again performed significantly better than the control at nearly all levels of water uptake; CaSt performed noticeably better than the Control and significantly worse than any of the other three additives. This graph again demonstrates the difference in performance between Control and tiles with additives and large amount of variance among samples for each treatment. In general, there is no statistically significant difference between the performance of NaSt, OleH, and CaOle additives under these conditions. In many cases, tiles with NaSt, OleH, and CaOle additives survived for over five months before reaching 50% mass increase, in striking contrast to the very best of the control samples, which lasted for only 72 hours.

The long-term viability of this material is dependent on how sensitive the properties are to available cardboard type. To understand the potential differences in water uptake between feedstocks, we prepared samples using three different cardboard sources: US corrugated cardboard (US Cardboard), paper plate discards from a factory in India (India Paper), and Chinet-brand paper plates purchased in the United States (US Plate).

 DOI: 10.7569/JRM.2016.634109

Figure 4 Epoxy-coated and scored samples, side and angled view. (**a**) Before immersion testing (0% mass gain). (**b**) During immersion testing, showing some swelling due to water uptake (20% mass gain). (**c**) After immersion testing and failure (50% mass gain).

For the first two, we prepared samples both with and without sodium stearate additive. Data comparing the water-uptake tests of these materials are found in Figure 6. Differences among the paper sources and the US Cardboard are small compared to the distinction between samples with and without additive and, in most conditions, are not statistically significant. This suggests that various cardboard feedstocks could be used to produce this material and that all would benefit from the use of a waterproofing additive of some variety.

3.2 Water Droplet Interactions with Material Surface

To better understand the interaction of water with the surface of our material, a device was constructed to take high-resolution photographs of a level material surface. This device was similar to those made for the measurement of contact angle of liquids on surfaces. However, irregularities in panel surfaces, especially protruding fibers, resulted in asymmetrical water drops and prevented precise measurement of contact angle and therefore calculation of surface free energy [35]. This is a common problem when working with fibrous, hydrophilic materials [39].

To provide a qualitative understanding of the behavior of this material, high resolution photographs were taken at 1 s, 5 s, 20 s, and 20 min times after a drop was dispensed. A clear difference in drop behavior among materials with different levels of additive was observed. Timed photo sets were taken using multiple panels of each type, and the image

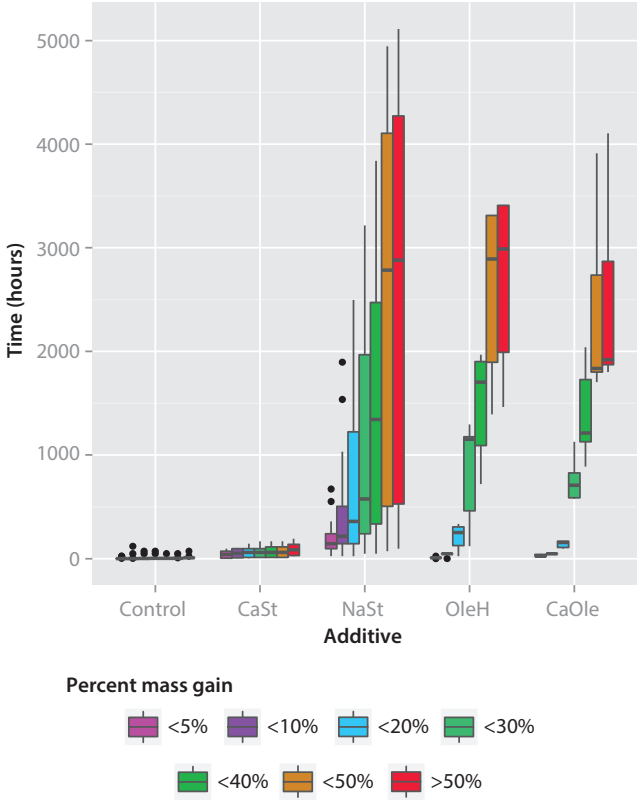

Figure 5 Mass increase vs. immersion time of 50 mm × 50 mm samples coated in epoxy and then scored, including a Control and NaSt, CaSt, OleH, and CaOle additives. Boxplots for each level of mass gain (denoted by color) and each additive treatment (grouped, labeled on x-axis) show median (line), second to third quartiles (box), most extreme data point within 1.5 × the interquartile range (whiskers), and outliers (black dots).

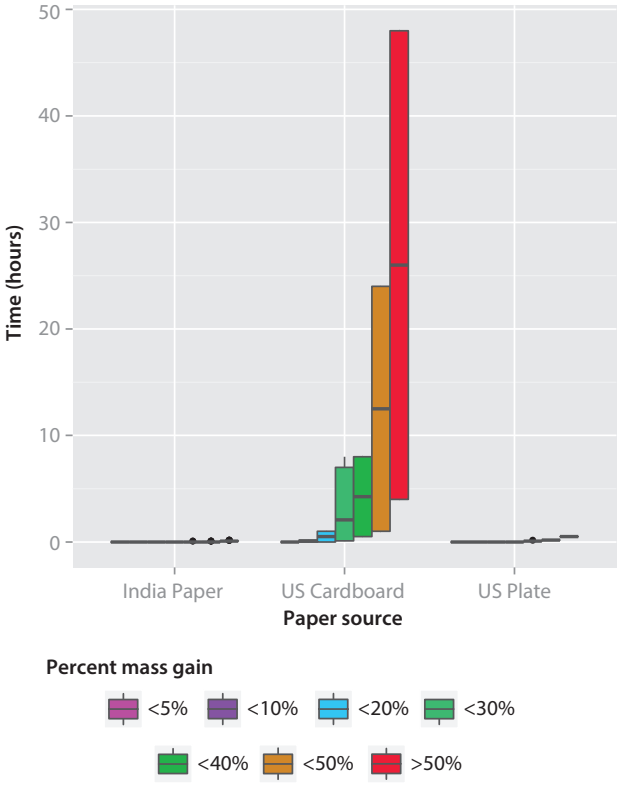

Figure 6 Mass increase vs. immersion time of 50 mm × 50 mm samples made from cardboard from three different sources: paper plates from India (India Paper), containerboard from the United States (US Cardboard), and paper plates from the United States (US Plate). Boxplots for each level of mass gain (denoted by color) and each additive treatment (grouped, labeled on x-axis) show median (line), second to third quartiles (box), most extreme data point within 1.5 × the interquartile range (whiskers), and outliers (black dots).

sets in Figure 7 are representative of all observations. Control panels showed immediate disappearance of the water drop, suggesting wetting of the surface and subsequent absorption by the porous material. Panels containing 2.13 kg/m^2 NaSt additive (sodium stearate and corresponding hydrochloric acid and calcium hydroxide) showed only marginally slower disappearance (and corresponding absorption). Panels containing 2.89 kg/m^2 NaSt additive showed a consistent droplet shape and almost no change in size after 20 minutes, suggesting that at higher levels, the additive imparts surface hydrophobicity to this material and prevents wetting and subsequent absorption. Given the porosity of the material (as contrasted with glass, which will "wet" but not absorb water), these observations of surface hydrophobicity are consistent with the apparent hydrophobicity of the bulk material observed in our measurements of bulk material water uptake.

3.3 Modulus of Rupture and Bending Modulus

Having demonstrated that additives significantly improve the water resistance of the material, it was important to understand any tradeoffs in terms of the mechanics of the material associated with the presence of additives. A four-point bending test in accordance with the ASTM D6272-10 Standard Test Method was used to record load-deflection curves for 152 mm by 305 mm samples of the material with various cardboard feedstocks and additives. From these curves the maximum flexural loads and maximum deflections for each sample were obtained and used to calculate the modulus of rupture (MOR) in bending (the stress in a cross section of the sample at the point of failure) and the modulus of elasticity in bending, also known as the bending modulus. The MOR and the bending modulus are only considered valid for failures located

 DOI: 10.7569/JRM.2016.634109

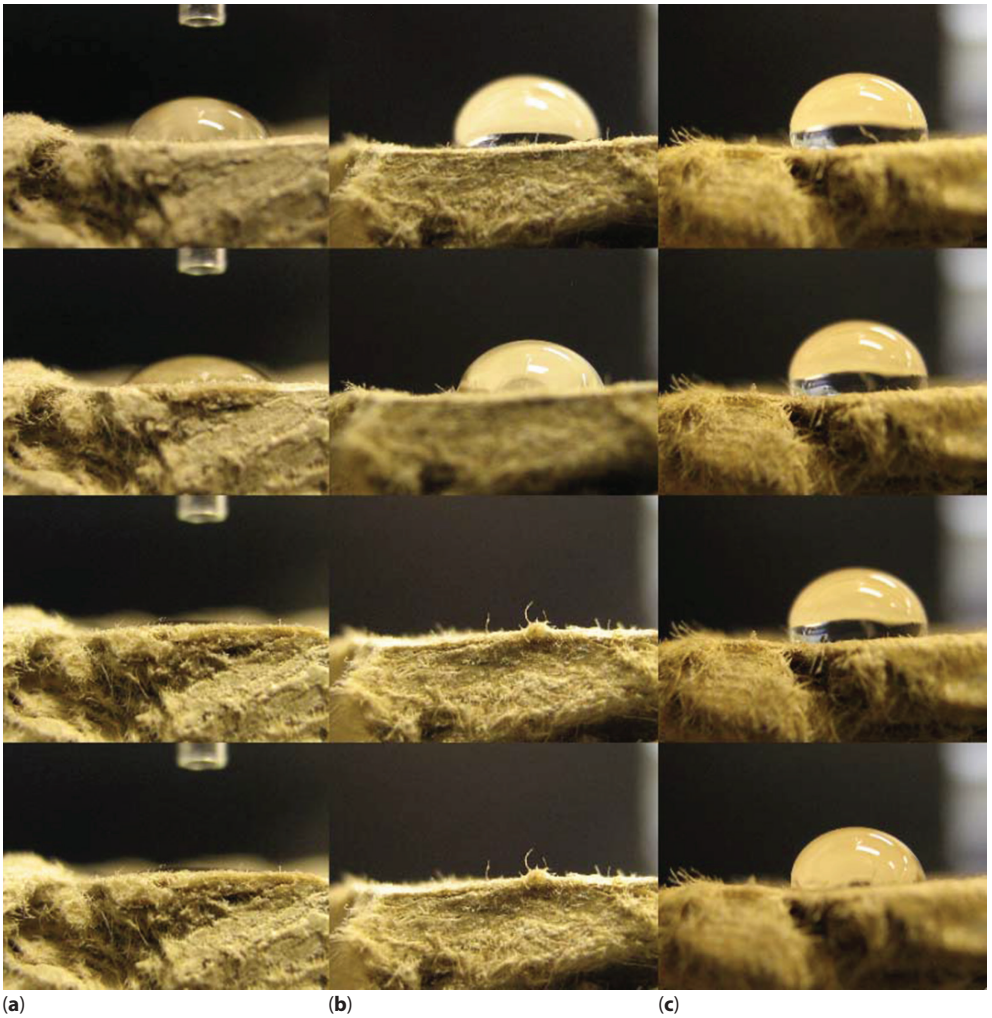

Figure 7 Drops of water after 1 second, 5 seconds, 20 seconds and 20 minutes after being deposited on (**a**) control panel, (**b**) 2.13 kg/m^2 NaSt panel, and (**c**) 2.89 kg/m^2 NaSt panel. The smaller drop size in (c) after 20 minutes is due to evaporation, with no panel wetting occurring.

in the center third of the sample by length, which is the region where failure was observed in all cases except one. The MOR was calculated with the assumption that samples were perfect rectangles with no warp and that during strength testing, the elastic modulus was linear up to the point of failure. Linear regression graphs of the load vs. deflection curves of our samples validated our assumption (see Supporting Information).

Figure 8 shows the MOR data for materials made from the India Paper feedstock with various additives. In general, additives reduced the strength of the material when compared to the control. Tiles containing CaSt, OleH, CaOle, and NaSt all had significantly lower values of MOR as compared to the Control but did not differ significantly from each other. On average, tiles containing additives had between 54% and 65% the MOR of the Control (7.25 MPa). The bending modulus did not vary significantly between additives or between samples containing additive and the Control.

The impact of feedstock choice on strength parameters, both with and without additive, was also tested to help understand the implications of this work in situations where access to cardboard feedstocks may vary. There were significant differences between the cardboard feedstock used in India (leftovers from a paper plate factory, India Paper), the paper plates sourced in the US (US Plate), and the general containerboard waste used in the US (US Cardboard). US Cardboard and US Plates yielded a composite with a significantly higher MOR than India Paper. In US Cardboard and India Paper samples, the NaSt additive decreased the MOR to 60% and 53% of the MOR of the Control samples, 5.61 and 7.25 MPa respectively. The MOR data for these samples are shown in Figure 9.

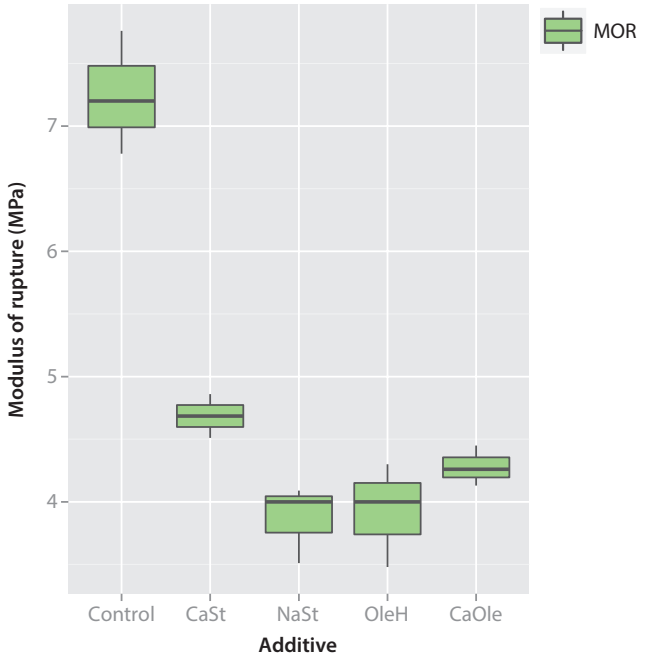

Figure 8 Modulus of rupture as calculated from the results of a four-point bend test of 152 mm × 305 mm samples including a Control and NaSt, CaSt, OleH, and CaOle additives. Boxplots show median (line), second to third quartiles (box), most extreme data point within 1.5 × the interquartile range (whiskers), and outliers (black dots).

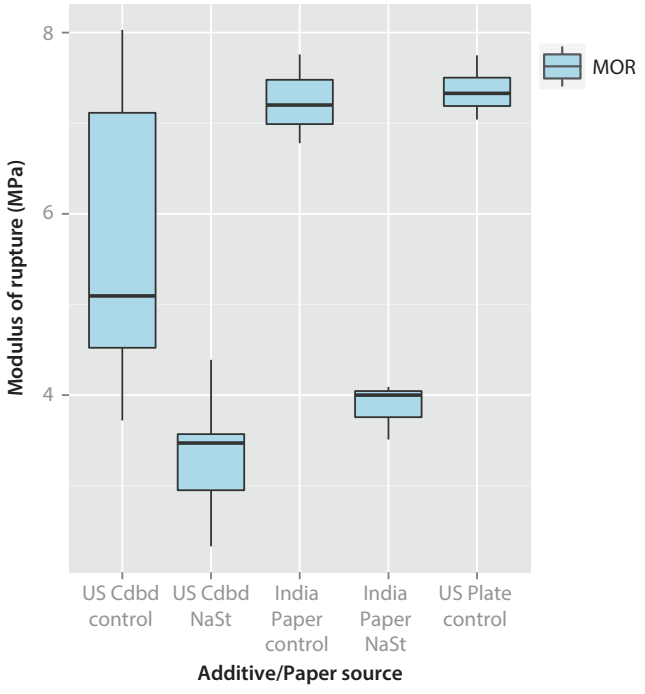

Figure 9 Modulus of rupture as calculated from the results of a four-point bend test of 152 mm × 305 mm samples from three different cardboard feedstocks, the first two with and without sodium stearate additive. Boxplots show median (line), second to third quartiles (box), most extreme data point within 1.5 × the interquartile range (whiskers), and outliers (black dots).

The bending modulus was again not impacted by the presence or absence of additive. The bending modulus was, however, impacted by cardboard feedstock. India Paper samples had higher bending moduli than either of the US feedstocks.

Commercially available samples of birch plywood, bullnose MDF (medium-density fiberboard), and MDF were tested using the same four-point bending test for comparison. The MOR of the cardboard control was roughly 31% that of the plywood (18.23 MPa), 41% that of bullnose MDF (13.761 MPa), and 13% that of MDF (43 MPa). The bending modulus of the cardboard control tile was similar to that of the birch plywood, but significantly lower than those of the Bullnose MDF and MDF samples. The values calculated for standard materials (18.23 MPa for plywood, 43 MPa for MDF) were comparable to those found in the literature (33.72–42.61 MPa for plywood, 35.85 MPa for MDF). This amount of variability in MOR is expected between experimental setups [40].

4 CONCLUSIONS AND FUTURE WORK

We have demonstrated that the addition of long-chain fatty acid salts to a new composite building material based on waste cardboard and a biobased binder provides significantly increased water repellency for these materials. The best additive, calcium oleate, increased the time to failure by nearly 900-fold in an uncoated "worst case scenario" immersion test and by over 160-fold in a more realistic test with water exposure of the material through a damaged waterproof coating. The best cases demonstrate that this material can survive with the vulnerable core exposed while submerged in water for over five months. The likely mechanism of this water-resistance is an interaction of the hydrophilic end of the molecule with the cellulose fibers of the cardboard and repellency with the hydrophobic end of the molecule. In addition to being water repellent in the presence of these additives, the material has a modulus of rupture that ranges between 3.3 MPa and 7.4 MPa and is weaker in the presence of waterproofing additives. Choice of cardboard feedstock had some impact on modulus of rupture and on some levels of water uptake, but the differences were small, suggesting that various cardboard feedstocks may be appropriate for use in this building material. The material is weaker than, but comparable to, plywood and MDF and has a similar bending modulus to plywood. Our work is ongoing to

understand the additional technical limitations of this material, such as durability and microbial resistance. While outside the scope of this work, cost of the material will ultimately be an important consideration as well. Additionally, a robust manufacturing process must be developed to address the high variability in water resistance observed in materials produced on a very small scale. We are working to determine in what markets this material may have the broadest impacts for improving material health in the built environment, both within Western regulatory frameworks and in developing economies.

ACKNOWLEDGMENTS

The authors are appreciative of assistance in Berkeley from Robert Spragg, Crysta Lynn Highfield, Cruz Carlos, Jeff Higginbotham and Matt Cataleta, as well as the students of the Haas Business School Cleantech to Market Course. The authors also thank Hasit Ganatra, Lisa von Rabenau, Sunny Gosain, Vikram Panchal, Prabha Brahman, Umiya Thakore, Nirvrat, Hitesh and others for their support in Ahmedabad, India.

This work was supported by the Development Impact Lab (USAID Cooperative Agreement AID-OAA-A-13-00002), part of the USAID Higher Education Solutions Network and by the US-India Science and Technology Endowment Fund.

REFERENCES

1. Government of India Ministry of Home Affairs, *Census of India 2011 - Primary Census Abstract Data for Slum*, http://www.censusindia.gov.in/2011census/population_enumeration.html (2011).
2. United Nations Human Settlements Programme (UN-HABITAT), *The State of the World's Cities 2006/7*, Earthscan Publications (2007).
3. International Agency for Research on Cancer, *Monographs on the Evaluation of Carcinogenic Risks to Humans - Asbestos (Chysotile, Amosite, Crocidolite, Tremolite, Actinolite, and Anthophyllite)*, **100C** Lyon, France (2012).
4. International Agency for Research on Cancer, *Monographs on the Evaluation of Carcinogenic Risks to Humans - Formaldehyde, 2-Butoxyethanol*, http://monographs.iarc.fr/ENG/Monographs/vol88/mono88.pdf (2006)
5. IBISWorld, *Global Cardboard Box & Container Manufacturing*, http://clients1.ibisworld.com/reports/gl/industry/default.aspx?entid=540 (2015).
6. G. H. D. Tonoli, *et al*., Surface properties of eucalyptus pulp fibres as reinforcement of cement-based composites. *Holzforschung* **64,** 595–601 (2010).
7. S. F. Santos, G. H. D. Tonoli, J. E. B. Mejia, J. Fiorelli, and H. Savastano Jr, Non-conventional cement-based composites reinforced with vegetable fibers: A review of strategies to improve durability. *Mater. Constr.* **65** (2015).
8. V. K. Thakur, M. K. Thakur, and R. K. Gupta, Review: Raw natural fiber–based polymer composites. *Int. J. Polym. Anal. Charact.* **19,** 256–271 (2014).
9. C. J. Biermann, *Essentials of Pulping and Papermaking*, Academic Press, Inc., San Diego, CA (1993).
10. Homasote green building boards – sound proof fiberboard. www.homasote.com (Accessed 2015).
11. Econovate - EconoBlok. www.econovate.com (Accessed 2015).
12. H. Ganatra, ReMaterials - High quality roofing for the developing world. re-materials.com (Accessed 2015).
13. C. Lin, *et al*., Food waste as a valuable resource for the production of chemicals, materials and fuels. Current situation and global perspective. *Energy Environ. Sci.* **6,** 426–464 (2013).
14. Strawtec Building Solutions - Made in Rwanda, www.strawtec.com (Accessed 2015).
15. J. Vallette, C. Murtagh, W. Sullens, and T. Lent, *Post-Consumer Polyvinyl Chloride in Building Products*, Healthy Building Network, Berkeley, CA (2015).
16. J. Vallette, T. Schettler, and M. Wolfe, *Asthmagens in Building Materials: The Problem and Solutions*, Conference Paper, Published by Greenbuild International Conference and Expo, New Orleans, LA (2014).
17. M. McGeehin, CDC Reports on Levels of Formaldehyde in FEMA Temporary Housing Units Supplied to Katrina Victims in the Gulf Coast (2008).
18. A. Bentur and S. A. S. Akers, The microstructure and ageing of cellulose fibre reinforced cement composites cured in a normal environment. *Int. J. Cem. Compos. Light. Concr.* **11,** 99–109 (1989).
19. M. J. John and R. D. Anandjiwala, Recent developments in chemical modification and characterization of natural fiber-reinforced composites. *Polym. Compos.* **16,** 187–207 (2008).
20. S. Mukhopadhyay and R. Fangueiro, Physical modification of natural fibers and thermoplastic films for composites – A review. *J. Thermoplast. Compos. Mater.* **22,** 135–162 (2009).
21. G. H. D. Tonoli, *et al*., Effects of Eucalyptus pulp refining on the performance and durability of fibre-cement composites. *J. Trop. For. Sci.* **25,** 400–409 (2013).
22. P. T. Anastas and J. C. Warner, *Green Chemistry: Theory and Practice*, Oxford University Press, Oxford (1998).
23. A. S. Singha and V. K. Thakur, Synthesis and characterizations of silane teated *Grewia optiva* fibers. *Int. J. Polym. Anal. Charact.* **14,** 301–321 (2009).
24. A. S. Singha and V. K. Thakur, Morphological, thermal, and physicochemical characterization of surface modified pinus fibers. *Int. J. Polym. Anal. Charact.* **14,** 271–289 (2009).
25. A. S. Singha and A. K. Rana, Improvement of interfacial adhesion in *Cannabis indica*/unsaturated polyester biocomposites through esterification reaction. *Int. J. Polym. Anal. Charact.* **17,** 590–599 (2012).
26. V. K. Thakur A. S. Singha, and M. K. Thakur, Surface modification of natural polymers to impart low water

absorbency. *Int. J. Polym. Anal. Charact.* **17,** 133–143 (2012).
27. A. S. Singha and R. K. Rana, Functional polymers from lignocellulosic materials: Synthesis, characterization, and evaluation of properties. *Int. J. Polym. Anal. Charact.* **17,** 499–514 (2012).
28. G. F. Fanta, R. C. Burr, and W. M. Doane, Graft polymerization of acrylamide and 2-acrylamido-2-methylpropanesulfonic acid onto starch. *J. Appl. Polym. Sci.* **24,** 2015–2023 (1979).
29. O. Paquet, M. Krouit, J. Bras, W. Thielemans, and M. N. Belgacem, Surface modification of cellulose by PCL grafts. *Acta Mater.* **58,** 792–801 (2010).
30. G. H. D. Tonoli, *et al*., Isocyanate-treated cellulose pulp and its effect on the alkali resistance and performance of fiber cement composites. *Holzforschung* **67,** 853–861 (2013).
31. L. Rueda, *et al*., Isocyanate-rich cellulose nanocrystals and their selective insertion in elastomeric polyurethane. *Compos. Sci. Technol.* **71,** 1953–1960 (2011).
32. J. Raabe, *et al*., Evaluation of reaction factors for deposition of silica (SiO2) nanoparticles on cellulose fibers. *Carbohydr. Polym.* **114,** 424–431 (2014).
33. D. C. Harris, *Quantitative Chemical Analysis*, 6th ed., pp. 61–79 Department of Agriculture, Forest Service, Forest Products Laboratory, Madison, WI (2003).
34. J. Yuan, G. Gu, S. Zhou, and L. Wu, Preparation and characterization of silicone-grafted styrene-butyl acrylate latex copolymer. *High Perform. Polym.* **16,** 69–80 (2004).
35. D. Kwok, T. Gietzelt, K. Grundke, and H. Jacobasch, Contact angle measurements and contact angle interpretation. 1. Contact angle measurements by axisymmetric drop shape analysis and a goniometer sessile drop technique. *Langmuir* **7463,** 2880–2894 (1997).
36. National Instruments, LabVIEW 7.1 (2004).
37. J. M. Gere, *Mechanics of Materials*, 5th ed., p. 895, Brooks/Cole Pacific Grove, CA (2001).
38. National Institute of Health U.S. National Library of Medicine, MedlinePlus - Allergies, asthma, and dust, https://www.nlm.nih.gov/medlineplus/ency/patientinstructions/000487.htm (Accessed 2015).
39. L. Černe, B. Simončič, and M. Željko, The influence of repellent coatings on surface free energy of glass plate and cotton fabric. *Appl. Surf. Sci.* **254,** 6467–6477 (2008).
40. N. M. Stark, C. Zhiyong, and C. G. Carll, Department of Agriculture, Forest Service, Forest Products Laboratory, http://www.fpl.fs.fed.us/products/publications/several_pubs.php?grouping_id=100 (Accessed 2015).

Supplementary Document Available Online

http://www.scrivenerpublishing.com/journalsuppl/jrm/JRM-2016-0021/JRM-2016-0021_supp.zip